The Effects of Doppler and Pulse Eclipsing on Sidelobe Reduction Techniques

Richard O. Lane
Centre for Signal and Information Processing
QinetiQ
Malvern, UK
rlane1@QinetiQ.com

***Abstract*—Radar sidelobe reduction techniques based on deconvolution generally rely on an accurate estimate of the system point spread function (PSF). Targets traveling at non-zero velocity induce a Doppler shift and have an altered PSF, which reduces sidelobe reduction performance. Also, in situations where a target is close to the radar, pulse eclipsing occurs – reflected energy arrives at the receiver while it is switched off during transmission. Eclipsing has the effect of a range-varying PSF, which also reduces sidelobe reduction performance. This paper describes a method to account for both Doppler and pulse eclipsing using the thresholded minimum mean square error (MMSE-T) sidelobe reduction algorithm. A new procedure for estimating noise power, which is required by the algorithm, is presented. Simulation results show the modified algorithm is able to reduce sidelobes such that a weak target obscured by the sidelobes of a 40 dB stronger target is clearly revealed, assuming the weak target would be detectable alone. These results hold when the true target velocities are not known as long as a reasonable estimate is obtained through tracking or Doppler processing of the strongest targets. A qualitative comparison of MMSE-T with the iterative re-weighted least squares (IRLS) algorithm shows it to be the better of the two.**

I. Introduction

Pulse compression is a technique used in radar systems to achieve both a high transmission energy and good range resolution by frequency or phase modulation of a long pulse. The optimal receiver filter, in terms of the peak-signal-to-mean-noise power ratio, is the matched filter with an impulse response that is a time-reversed copy of the transmitted waveform [1]. A consequence of the filtering process is the production of range sidelobes, which mask weak targets in the presence of stronger ones. Although amplitude weighting may be used in the receive filter to reduce sidelobes the weighting process increases the width of the main lobe and further techniques are required to achieve an improved detection performance, while maintaining resolution.

Algorithms that attempt to remove the effect of the system point spread function (PSF) are known as deconvolution or super-resolution algorithms. The performance of these algorithms depends critically on the level of noise in the system and the accuracy with which the PSF is known. Two phenomena that alter PSFs are target Doppler shifts and pulse eclipsing. If a target is moving then the Doppler shift induced in the signal received by the system alters the PSF – an effect characterized by the waveform ambiguity diagram [1]. Although Doppler processing or target tracking can provide corrections for target velocity, residual errors will remain resulting in a non-ideal PSF with a reduced peak power and a broadened main lobe. Pulse eclipsing occurs due to the receiver being switched off while the system is transmitting another pulse; therefore the entire waveform will not be received for targets that are very close to the transmitting system [2] or near the end of the range-unambiguous extent. This results in a degradation of the PSF similar to the Doppler effect. Eclipsing is a particular problem in systems with a high duty ratio, where the length of the pulse is large compared to the pulse repetition interval, because a large proportion of the range profile will be eclipsed.

The remainder of the paper is organized as follows. Section II describes a model for the pulse compression system, including Doppler and eclipsing effects, and introduces the thresholded minimum mean square error (MMSE-T) sidelobe reduction algorithm. Section III presents results of the algorithm on a variety of simulated scenes. Section IV introduces and shows results of a new procedure to estimate noise power, which is required by the algorithm. Finally conclusions are drawn in section V.

II. System Model and Algorithms

A. Introduction

The output of a matched filter is the convolution of the PSF and the underlying target scene. This convolution may be written in matrix form:

$$g = Tf + n, \tag{1}$$

where f is an $N\times1$ vector containing the sampled complex backscatter coefficient of the scene as a function of distance,

This work was funded by the UK Ministry of Defence "Technology for Phased Array Radar (ARTIST Support)" Principal Programme

T is an $N \times N$ complex matrix whose columns contain shifted versions of the system PSF, n is an $N \times 1$ Gaussian distributed random complex vector representing system noise and g is an $N \times 1$ vector containing the range profile. Where a target at a particular range cell has a non-zero Doppler frequency the corresponding column of T is replaced by the appropriate sampled vector from the waveform ambiguity function. Near-range eclipsing effects are modeled by replacing the columns at the left hand side of T with the eclipsed point response. Far-range eclipsing has not been addressed to date but would require a change in the columns of T at the right-hand side in a similar manner to near-range eclipsing.

Many algorithms have been proposed to obtain an estimate of the scene f, given the measured range profile g. The process is known as deconvolution or super-resolution. This paper considers the sidelobe reduction properties of deconvolution as an aid to target detection. A study comparing the algorithms: matrix pseudo-inverse, also known as least-squares or LS, singular value decomposition (SVD), thresholded minimum mean square error (MMSE-T) and multiple signal classification (MUSIC) found MMSE-T to be the most robust algorithm for 2D super-resolution of ISAR images [3]. This algorithm was originally reported in [4] and later clarified in [5]. A different version of MMSE, termed pulse compression repair (PCR), has recently been proposed and has been tested in simulations where the target appears in the eclipsed region [6] and Doppler effects occur [7]. However, the specific effects of eclipsing and Doppler were not included in the model for scene estimation *i.e.* in determining the amplitude of targets or clutter at every sample point. Separate attempts by Zejak *et al*. to reduce degradation due to both eclipsing [2] and Doppler [8] have been made using a modified version of the matrix inverse called iterative re-weighted least squares (IRLS). As the MMSE-T algorithm has been shown to be superior to the basic matrix inverse we propose in this paper to use Doppler and eclipsing models in the MMSE-T algorithm to improve performance over the IRLS algorithm.

B. The MMSE-T algorithm

If the covariance matrix of the prior distribution of the underlying scene f is W and the noise covariance matrix is N_C then the solution for f that minimizes the mean square error is given by [4] [5] [9]:

$$f_{\mathrm{MMSE}} = WT^H(TWT^H+N_C)^{-1}g. \qquad (2)$$

However, in general W is not known in advance because prior knowledge of the scene is not well defined. Therefore an iterative scheme that updates the W matrix is used [4]. In this scheme W is set to the identity matrix for the first iteration and in subsequent iterations is estimated from the current estimate of f. Any element of f whose power is below a threshold is assumed to be clutter and the combined variance of all these elements is calculated and entered into W at the appropriate points. Any element i above the threshold has its variance set to $|f_i|^2$. Therefore W is always diagonal and has a high variance where there is a valid target or a large scatterer. The procedure is repeated by alternately estimating W and f until a termination criterion is met when f changes by less than a specified amount between iterations.

The MMSE-T algorithm is versatile and can be used in any situation where the model in (1) applies and the PSF T is known. It has been applied to focused and unfocused SAR images in [9] where the defocus was simulated from aircraft movement spectra. An analytical derivation of the effect of cross-track acceleration on the algorithm was presented in [10]. ISAR images have also been used to test MMSE-T super-resolution in [3]. To the author's knowledge there are no examples in the open literature where the algorithm has been applied to range profiles. Also, the MMSE-T solution has not previously used information about target Doppler and pulse eclipsing, which can simply be encoded in the T matrix of the solution without altering the basic algorithm.

If two or more targets with different Doppler shifts were present in the same range bin then full Doppler processing would be required to produce a range-Doppler map. The g and f vectors would be raster scanned versions of the measured 2D range-Doppler map or estimated scene. The T matrix would represent the ambiguity function and be appropriately block formatted as for the SAR/ISAR cases above. This situation has not currently been simulated.

III. Simulation Results

A. Doppler Effect

In the following scenarios the waveform used for all simulations was a linear frequency modulated (FM) pulse with a 5 MHz bandwidth and a 3 μs pulse length. The pulse repetition frequency (PRF) does not affect the results as long as it is high enough to determine the target velocity unambiguously, if Doppler processing is used.

The first simulation tests the situation where a weak target is hidden by the presence of matched-filter sidelobes from a stronger target as shown in Fig. 1. The signal-to-noise ratio (SNR) for the stronger target is 70 dB. This target has a Doppler shift of 2 kHz applied to it, which corresponds to a velocity of 100 ms^{-1} or 194 knots at a radar centre frequency of 3 GHz. The signal-to-clutter ratio (SCR) is 60 dB with the clutter having a zero Doppler shift. The weak target has a power of -40 dB relative to the strong target and also a zero Doppler shift. Fig. 1 shows that the MMSE-T algorithm has reduced the sidelobe levels and revealed the weak target even though the algorithm did not use knowledge of the stronger target's Doppler.

The second case (Fig. 2) repeats the experiment with the stronger target having a Doppler shift of 6.6 kHz (330 ms^{-1}). Here we see that, while the algorithm has generally reduced the sidelobe levels, the increased target speed has resulted in spurious peaks that would reduce the ability to detect the weak target without an unacceptably high false alarm rate.

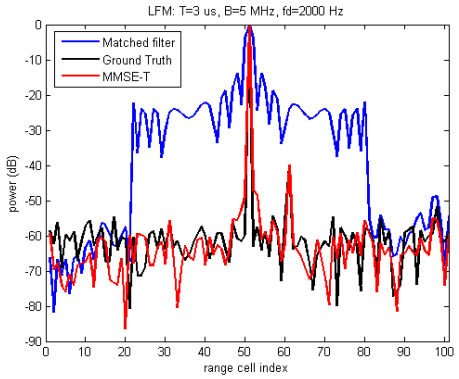

Figure 1. True stronger target Doppler 2 kHz, assumed Doppler zero

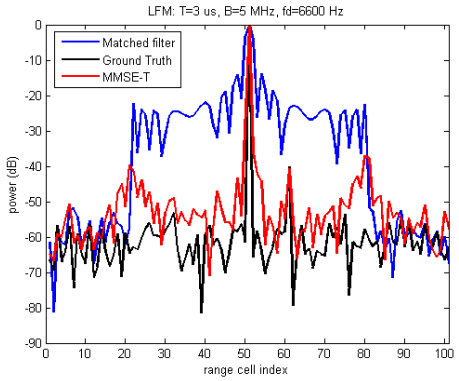

Figure 2. True stronger target Doppler 6.6 kHz, assumed Doppler zero

In many systems an estimate of target velocity for strong targets will be available through tracking or Doppler processing. This velocity estimate can be used to aid the MMSE-T algorithm in determining the scene. The process is illustrated in Fig. 3, where the true stronger target velocity is 330 ms^{-1} (6.6 kHz) but it has been assumed that the target is moving at 220 ms^{-1} (4.4 kHz). This is taken as an extreme case as it is unlikely an estimated target velocity will be in error by this amount. We see that even though the velocity estimate is incorrect the algorithm has been successful in achieving very low sidelobe levels and the second target has been revealed. As the accuracy of the velocity estimate decreases the MMSE-T estimate of the scene will degrade. The point at which target velocity becomes an issue will vary depending on the bandwidth of the pulse.

B. Eclipsed Zone

In the following scenarios the waveform used for all simulations was the same as the previous section: a linear FM pulse with a 5 MHz bandwidth and a 3 µs pulse length. Near-range eclipsing has been taken into account by modification of the PSF matrix *T*. The duty ratio of the waveform is not critically important to the results – high duty waveforms will have a larger proportion of the range profile in the eclipsed zone but this should not significantly degrade performance as will be demonstrated. These results should also hold for other types of waveform.

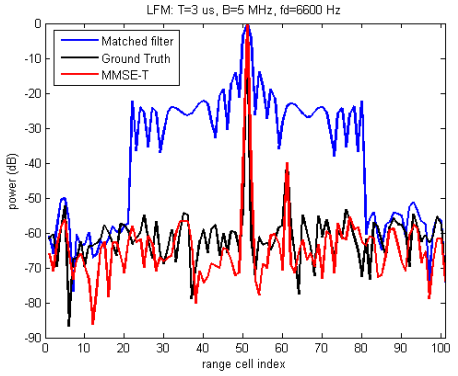

Figure 3. True target Doppler 6.6 kHz, assumed target Doppler 4.4 kHz.

Fig. 4 shows a situation where two targets with relative powers 0 dB and -40 dB are in the un-eclipsed zone and a third target with relative power -20 dB is in the eclipsed zone. The level of eclipsing varies linearly from 100% eclipsed at range cell index 1 to 0% eclipsed at range cell index 30. The simulated matched filter output has taken this eclipsing effect into account but this information was not provided to the MMSE-T algorithm. The recovered scene has peaks relating to each of the three targets but the weakest target has a reduced power and the target in the eclipsed zone has both a reduced power and broad main lobe. The high resultant background noise level would make detection of the -40 dB target difficult. Fig. 5 shows the results when eclipsing has properly been accounted for and all three targets are easily detectable.

The reason the effect of pulse eclipsing can be compensated fully is that eclipsing is a deterministic effect – the eclipsed response as a function of distance is known in advance. This means the duty ratio does not have a large effect on side-lobe reduction performance. However, there will be a penalty in performance due to the decreased signal-to-noise ratio because the entire signal has not been received. If too large a portion of the pulse on a target is eclipsed the SNR will be insufficient for the algorithm to determine that the target is not a noise spike.

As a final test of the algorithm Fig. 6 shows a scene containing several targets with velocities varying between zero and 100 ms^{-1} including two targets in the eclipsed zone. Target velocity information was not passed to the algorithm. The MMSE-T algorithm successfully reduces sidelobe levels, although there is a higher residual background noise/clutter level for this more challenging scenario.

It may be observed that in addition to a reduction in sidelobe levels the resolution has improved over that of the matched filter. This is because the MMSE-T algorithm is a deconvolution algorithm – it attempts to remove all effects of the point spread function including the width of the main lobe. Under ideal conditions the algorithm provides a resolution improvement factor of r_r/r_s, where r_r is the original range resolution and r_s is the distance between range sampling points.

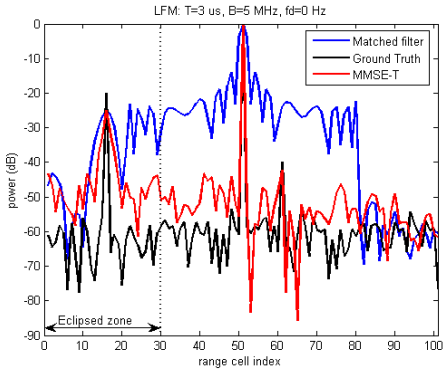

Figure 4. Target in eclipsed zone, eclipsing not taken into account

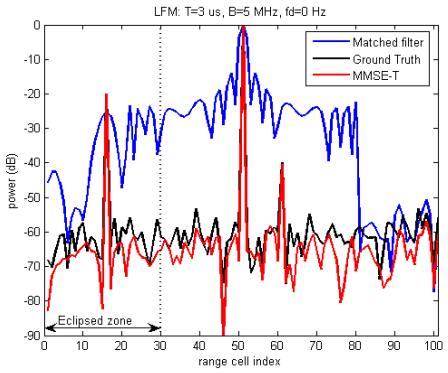

Figure 5. Target in eclipsed zone and fully accounted for

Since the matched filter is optimum in terms of the peak-signal-to-mean-noise power ratio it will maximize detection performance for the strongest target in a range profile (or group of targets, if separated by less than the system resolution), although performance is not necessarily optimum for other weaker targets. Therefore if the entire detection process is carried out after scene estimation using the MMSE-T algorithm there is a drop in performance for the strongest target but a potential improvement for other targets. Therefore it is recommended that an initial detection stage is used to detect the strongest target using a matched filter. If the strongest target is detected then the MMSE-T algorithm can be applied and there will be no detection loss as the peak target has already been detected. If the strongest target cannot be detected in the matched filter response then the signal-to-noise ratio will be too small for useful application of the MMSE-T algorithm.

IV. ESTIMATING NOISE POWER

A. *Introduction*

The MMSE-T algorithm requires knowledge of the PSF and the mean noise power. The PSF may be estimated using knowledge of the signal bandwidth and the window function used in the matched filter to reduce sidelobes. Alternatively once a radar has been built the PSF may be measured by recording data from a strong point scatterer, such as a trihedral reflector.

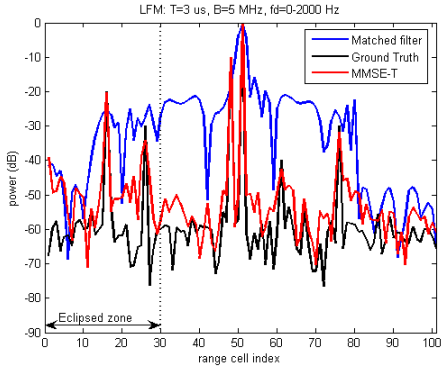

Figure 6. Multiple targets with high Doppler and in eclipsed zone

While there may be some drift over very long periods of time, the PSF should remain reasonably constant. The noise power in the system is initially modeled as thermal noise in the radar receiver, which is filtered during the matched filter process. This noise level depends on the temperature of the receiver, so in theory if the temperature is known then the noise power can be calculated. However, in practice the noise term should include effects such as transmit/receive non-linearities, phase disturbances and other spurious effects that have not been taken into account in the model. This would particularly be the case for wideband radar.

If the assumed noise level is set too low then the algorithm tries to over-fit the data resulting in an estimated scene with alternate pixels having very strong powers but opposite phase. The smoothing effect of the PSF T tends to cancel these out and produce a range profile or image close to that of the measured data g. The estimated scene, however, would not be an accurate representation of the true scene. If the assumed noise is too large then the estimated scene will consist of very few point targets regardless of whether the scene contains point or distributed targets, or clutter. This is because any deviation from a perfect PSF in the measured data will be assumed to be noise rather than target structure.

Since non-thermal noise effects are either unknown or cannot be measured it may be necessary to estimate total system noise from the data themselves. An automatic method for doing this is now described.

B. *Estimation Algorithm*

The signal generation model is shown in (1). For a given estimate of the underlying scene f_{est} an estimate of the mean noise power in each range bin is:

$$\sigma^2_{\text{est}} = 1/N \times \| T f_{est} - g \|^2, \quad (3)$$

where N is the number of bins in the range profile. This procedure was carried out with a scene containing the targets shown in Fig. 6 and a noise power of -30dB relative to the strongest target. The target Doppler shifts were assumed to be known. Fig. 7 shows a plot of the estimated noise power against the assumed noise power given to the algorithm. The

graph was generated by multiple runs of the algorithm, each time assuming a noise power in the range -140 to 40 dB, estimating f using the MMSE-T algorithm and then estimating the noise power according to (3). The line of self-consistency in this graph is given where the estimated noise is equal to the assumed noise level. It can be seen that for this scenario the algorithm is approximately self-consistent for a range of noise power levels from -30 dB to -45 dB, which includes the true value of -30 dB.

If the assumed noise standard deviation is σ_{in}, a measure of self-consistency can be defined as:

$$SC = \begin{cases} \sigma_{est} / \sigma_{in} & \sigma_{est} \le \sigma_{in} \\ \sigma_{in} / \sigma_{est} & \sigma_{est} > \sigma_{in} \end{cases}, \quad (4)$$

which lies in the range $0 \le SC \le 1$ and reaches a maximum when the input and estimated noise power levels are equal. A plot of this measure for a set of input noise levels is shown in Fig. 8. If one were to use this metric as the sole basis for estimating the true noise level then there is an ambiguity: should it be set at -30 dB or -45 dB?

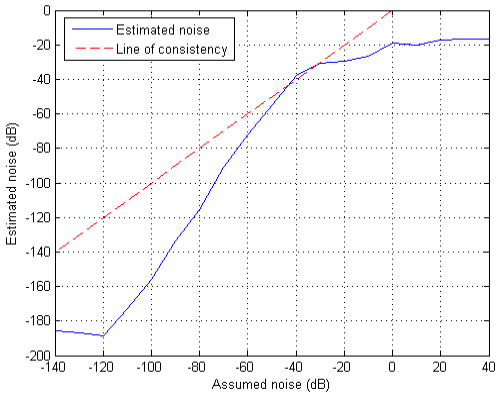

Figure 7. Estimated vs. assumed noise level for the simulated multiple target scenario shown in Figure 4.

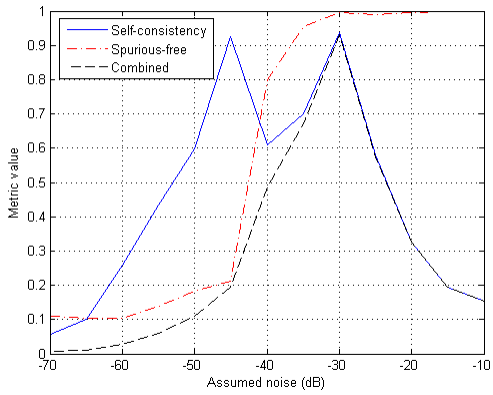

Figure 8. Optimising the assumed noise level

Another way of determining whether the data have been over-fitted is to compare the power of the estimated scene and the measured range profile. If the PSF T is normalized to have unit maximum value then in general for any particular pixel it is expected that the magnitude of the measured profile will be higher than the true scene. This is because the value of a pixel in the measured profile is the sum of the true scene at that point and the effect of other points due to the spatial spreading nature of the PSF. While it is possible to have lower measured values due to coherent combination of different elements of the true scene or the addition of noise that cancels out the true scene, these effects would in general involve a small proportion of pixels. When the data are over-fitted alternate pixels of the estimated scene have a spurious strong magnitude of opposite phase and often have a larger magnitude than the measured data. This can be quantified by defining a spurious-free measure that is equal to one when the estimated scene power is less than the measured power; otherwise it is given by the ratio of the measured and estimated powers. This metric is also in the range of zero to one and is mathematically given by:

$$SF_{pixel}(i) = \begin{cases} 1 & \dfrac{|f_{est}(i)|}{|g(i)|} \le 1 \\ \dfrac{|g(i)|}{|f_{est}(i)|} & \dfrac{|f_{est}(i)|}{|g(i)|} > 1 \end{cases}. \quad (5)$$

The measure for the whole scene is the mean over all pixels:

$$SF = \frac{1}{N} \sum_{i=1}^{N} SF_{pixel}(i). \quad (6)$$

When SF is close to unity the data have not been over fitted. A plot of SF against the assumed noise level is shown in Fig. 8. For high assumed noise levels SF is equal to 1. As the noise level is reduced a point is reached just below the true noise level of -30 dB where SF rapidly drops to about 0.1 where it remains for all low noise levels. This demonstrates the SF metric is good at rejecting low assumed noise levels that result in a spurious estimated scene.

A total combined quality metric may be defined as the product of the self-consistency and spurious-free measures:

$$CQ = SC \times SF. \quad (7)$$

The combined metric is plotted in Fig. 8, where it has an unambiguous peak at the true noise value of -30 dB. This procedure for estimating noise power has been repeated for a variety of true noise levels and scenes containing different numbers of targets and is consistent in estimating the true noise power to within a few dB.

The advantage of using this technique is that it is possible automatically to determine the true noise level, where previously it had to be set manually. The disadvantage is the extra processing cost. The MMSE algorithm itself is of order N^3 which can result in long processing times for large images or range profiles. The procedure to estimate noise requires a

full MMSE run for each assumed noise level tested. In practice, it is only necessary to know the noise power to an accuracy of about 10 dB. Therefore for a 100 dB range of tested noise levels the procedure would result in a slow-down factor of 10. However, when implemented in a real system the noise levels are unlikely to change significantly from pulse to pulse so the procedure need only be repeated every M pulses. In that case the additional processing load for noise estimation would be $10/M$, which would not be significant for large M.

V. CONCLUSIONS

The MMSE-T algorithm is able to significantly reduce sidelobes produced in the matched filtering process, enabling the detection of weak targets in the presence of strong ones. Performance of the algorithm is reduced when targets are moving with a very high velocity or are present in the eclipsed region. If an estimate of strong target velocities is available then the algorithm may make use of this to recover initial performance. The deterministic effect of pulse eclipsing may be taken into account to reduce performance loss. Comparing simulation results in this paper with those of [2] shows MMSE-T to be an improvement over the IRLS algorithm.

Many other deconvolution algorithms follow the signal generation model shown in (1). These algorithms would also be able to use target velocity and eclipsing information to improve performance under conditions where those effects are significant. The fundamental limit to all the algorithms is reasonable knowledge of the PSF and sufficient SNR.

ACKNOWLEDGMENTS

The author would like to thank colleagues at QinetiQ Malvern for helpful comments on the draft manuscript. Continuing support of the EPSRC Engineering Doctorate scheme is also acknowledged.

REFERENCES

[1] M. I. Skolnik, Introduction to radar systems, McGraw-Hill, 1980.

[2] B. M. Zrnic, A. J. Zejak, I. S. Simic, Target detection enhancement for the chirp radar in the eclipsing zone, IEEE 6th International symposium on spread spectrum techniques and applications, Vol. 1:269-273, 2000.

[3] R. O. Lane, K. D. Copsey, A. R. Webb, Assessment of a Bayesian approach to recognising relocatable targets, NATO RTO SET-096 specialists' meeting on the millimeter-wave advanced target recognition and identification experiment (MATRIX 2005), Oberammergau, Germany, 10-12 May 2005.

[4] S. P. Luttrell and C. J. Oliver, Prior knowledge in synthetic-aperture radar processing, J. Phys. D: Appl. Phys. 19, pp. 333-356, 1986.

[5] L. M. Delves, G. C. Pryde, and S. P. Luttrell, A super-resolution algorithm for SAR images, Inverse Problems 4(3), pp. 681-703, 1988.

[6] S .D. Blunt, K. Gerlach, A novel pulse compression scheme based on minimum mean-square error reiteration, International Conference on Radar, Adelaide, Australia, 3-5 September 2003.

[7] S. D. Blunt, K. Gerlach, Adaptive Pulse Compression Repair Processing, International Radar Conference, Arlington, Virginia, 9-12 May 2005.

[8] A. J. Zejak, E. Zenter, P. B. Rapajić, Doppler optimised mismatched filters, Electronics Letters 27(7):558-560, 1991.

[9] D. Blacknell and S. Quegan, SAR super-resolution using a perturbed point spread function, IGARSS, pp. 2592-2595, July 1989.

[10] R. O. Lane, Super-resolution and the radar point spread function, Proceedings of the London Communications Symposium, pp. 5-9, September 2005.